Available online at www.sciencedirect.com
ScienceDirect
Catalysis Today 133–135 (2008) 292–298
CATALYSIS TODAY
www.elsevier.com/locate/cattod

Hydrodesulfurization of 4,6-dimethyldibenzothiophene over Co(Ni)MoS_2 catalysts supported on alumina: Effect of gallium as an additive

Efraín Altamirano [a,b], José Antonio de los Reyes [a], Florentino Murrieta [c], Michel Vrinat [b,*]

[a] *Universidad A. Metropolitana-Iztapalapa, Área de Ingeniería Química, Av. FFCC R. Atlixco No. 186, Col. Vicentina, Iztapalapa, 09340 México, D.F., Mexico*
[b] *Institut de Recherches sur la Catalyse, 2 Av. A. Einstein, 69626 Villeurbanne Cedex, France*
[c] *Instituto Mexicano del Petróleo, Eje Central Lázaro Cárdenas 152, 07730 México, D.F., Mexico*

Available online 1 February 2008

Abstract

The effect of gallium over $CoMo/Al_2O_3$ and $NiMo/Al_2O_3$ catalysts was investigated in the hydrodesulfurization of 4,6-dimethyldibenzothiophene. The γ-Al_2O_3 support was modified, before the catalyst preparation, by impregnation with an aqueous solution of $Ga(NO_3)_3{\cdot}8H_2O$ and calcined at 450 °C. The catalytic results were correlated to the catalysts physicochemical properties which were obtained by different characterization techniques such as X-ray diffraction, X-ray Photoelectron Spectroscopy, Transmission Electron Microscopy and Diffuse Reflectance Spectroscopy. A change of the promoter (Co^{2+} or Ni^{2+}) interaction with the support is induced by the affinity of gallium (at low loadings) for the tetrahedral sites of alumina, leading to an increase in the octahedral species of Ni or Co. This improves the decoration of the MoS_2 slabs. Gallium also modifies the interaction of MoS_2 with the support, decreasing the numbers of Mo–O–Al anchors and increasing the stacking of the MoS_2 slabs. These modifications improve the activity of the NiMo and CoMo catalysts in the deep HDS of 4,6-DMDBT.

Keywords: Ga_2O_3; Al_2O_3; NiMo; CoMo; Hydrodesulfurization; 4,6-Dimethyldibenzothiophene; XPS; UV–vis

1. Introduction

The environmental regulations have forced the oil industry to reduce the sulfur content in gas oil cuts; one of the highest challenges in many countries is to improve the quality of diesel which nowadays should contain less than 50 ppm of sulfur and for the 2009 10 ppm. This sulfur reduction implies a great effort on the research in hydrotreatment catalysts (HDT). The most common HDT catalysts consist of an active phase of molybdenum sulfide (MoS_2) promoted by nickel (Ni) or cobalt (Co) usually supported on alumina (γ-Al_2O_3). The supported $CoMo/Al_2O_3$ (CoMo) catalyst is generally accepted to be excellent for the hydrodesulfurization (HDS), while the $NiMo/Al_2O_3$ catalyst shows a great activity in the hydrodenitrogenation (HDN) and hydrogenation (HYD), depending on the reaction conditions. The amount of molybdenum is normally between 10 and 14 wt% and the promoter is adjusted to an atomic relation of promoter/(promoter + Mo) optimized at 0.3 [1,2].

It has been observed that a trivalent additive such as gallium (Ga^{3+}) presents a high affinity for the alumina tetrahedral sites and, depending on the calcination temperature, this metal provokes changes on the promoter coordination (tetrahedral/octahedral) ($Ni^{2+}_{th}/Ni^{2+}_{Oh}$ or $Co^{2+}_{th}/Co^{2+}_{Oh}$) [3–5]. The boron ($B^{3+}$) has been largely studied as a trivalent additive in the CoMo catalysts, and the more accepted results suggest that B^{3+} has a positive effect over the molybdenum dispersion [6,7] and over the acidic properties of the support [8–11]. On the other hand, Jacono et al. [3,4] suggested that, depending on the impregnation sequence and on the metal loadings, Ga^{3+} increases the $Ni^{2+}_{th}/Ni^{2+}_{Oh}$ ratio on the Ni/Al_2O_3 catalyst, while the Ga^{3+} decreases the $Co^{2+}_{th}/Co^{2+}_{Oh}$ ratio on the $CoMo/Al_2O_3$ catalyst. In a recent paper [5] the positive gallium effect at low

* Corresponding author.
E-mail address: michel.vrinat@catalyse.cnrs.fr (M. Vrinat).

0920-5861/$ – see front matter
doi:10.1016/j.cattod.2007.12.085

loadings ($\leq$1.2 wt%) over the $Ni^{2+}_{th}/Ni^{2+}_{Oh}$ ratio has been reported; such an effect improves the activity of the NiMo catalyst on the HDS of 4,6-DMDBT. The aim of this work was to report new evidences which let us to understand the effect of gallium over the NiMo and CoMo catalysts on the HDS of 4,6-DMDBT.

2. Experimental

2.1. Catalyst preparation

The impregnation of gallium, molybdenum, nickel or cobalt was carried out by pore filling of a commercial γ-Al_2O_3 (high purity, BET surface area 240 $m^2\,g^{-1}$, pore volume (V_p) 0.63 $cm^3\,g^{-1}$ and particle size 80–100 μm) with the corresponding aqueous solutions. In the first impregnation ($Ga(NO_3)_3{\cdot}8H_2O$, Aldrich Chemical) the solids were calcined at 450 °C, and in the second impregnation (consecutive impregnation) the catalysts were calcined at 400 °C. The preparation and activation of the catalysts has been explained elsewhere [5]. The nomenclature is given in Table 1.

2.2. Catalytic activity tests

The HDS of 4,6-DMDBT was carried out in a three-phase continuous flow microreactor using a solution in dodecane (2.82×10^{-5} mol of 4,6-DMDBT into 300 ml of dodecane, corresponding to 300 ppm of S). The reaction conditions were: P_{H_2} = 3 MPa, H_2 flow = 2.6 $cm^3\,min^{-1}$, and the catalyst weight was approximately 50 mg. During the catalytic tests, two liquid flows were used with the aim to avoid high conversions (lower than 20%): F1 = 5.71×10^{-5} mol min^{-1} at 280, 300 and 320 °C, and F2 = 8.25×10^{-5} mol min^{-1} at 300, 320 and 340 °C. In all tests the two flows were programmed. The products were analyzed each 60 min by GC.

The specific reaction rates were calculated according to the following expression:

$$r = \frac{F}{m}(\mathrm{Conv}_{\mathrm{DBT's}}) \quad (1)$$

where r is the specific rate of disappearance of 4,6-DMDBT (mol $g^{-1}\,s^{-1}$), F is the molar flow rate of the reactant (mol s^{-1}), $\mathrm{Conv}_{4,6\text{-DMDBT}}$ is the conversion of 4,6-DMDBT, and m is the catalyst weight (g). All rates were estimated at low conversion (<20%).

2.3. Characterization techniques

After the final calcination, the metal contents were determined by atomic absorption after appropriate dissolution of the solids samples, and the results are presented in Table 1.

The XRD patterns of the calcined catalysts were recorded on a Bruker D5005 diffractometer using Cu Kα1 + α2 radiation (0.15418 nm) from 3 to 80° with 0.02° step size and 1 s at every step.

XPS measurements were performed on a VG Instrument type ESCALAB 200R spectrometer equipped with an Al Kα source ($h\nu$ = 1486.6 eV). The shifts of the peaks core line due to the charge of the sample were corrected by taking the Al 2p line of the catalyst support, γ-Al_2O_3 (Al 2p = 74.0 eV) as a reference. The sample holder was then transferred into the preparation chamber of the XPS equipment and it was passed into the analysis chamber after evacuation overnight (10^{-9} Pa).

The High Resolution Transmission Electron Microscopy (TEM) was performed with a 200 kV JEOL 2010 microscope, with a point resolution of 0.196 nm (coefficient of spherical aberration Cs = 0.5 mm). Freshly sulfided samples were ground under an inert atmosphere and were ultrasonically dispersed in ethanol. The suspension was collected on carbon-coated grids.

Diffuse Reflectance Spectroscopy was carried out with a PerkinElmer 580 (disperser) apparatus, working on diffuse reflectance mode. The acquisitions were done under 1000–200 nm domain, with a scan rate of 4 nm s^{-1}.

3. Results

3.1. Catalytic test

Table 2 shows the catalytic results of the HDS of 4,6-DMDBT over the NiMo catalysts with different amounts of

Table 1
Metal content and nomenclature of prepared catalysts

Catalyst	Nomenclature	Real (wt%)			Atoms nm^{-2}			Atomic ratio[a]
		Mo	Co (Ni)	Ga	Mo	Ni (Co)	Ga	
NiMo/γ-Al_2O_3	NiMo	9.9	2.3	0	2.8	1.0	0	0.25
NiMo/0.6Ga/γ-Al_2O_3	0.6NiMo	9.5	2.3	0.6	2.7	1.0	0.2	0.27
NiMo/1.2Ga/γ-Al_2O_3	1.2NiMo	9.0	2.2	1.2	2.5	0.9	0.4	0.26
NiMo/1.8Ga/γ-Al_2O_3	1.8NiMo	9.5	2.3	1.9	2.7	1.0	0.7	0.27
NiMo/2.9Ga/γ-Al_2O_3	2.9NiMo	9.6	2.3	2.8	2.7	1.0	1.0	0.27
NiMo/5.9Ga/γ-Al_2O_3	5.9NiMo	9.1	2.1	6.5	2.5	0.9	2.2	0.26
CoMo/γ-Al_2O_3	CoMo	9.2	2.3	0	2.6	1.0	0	0.28
CoMo/0.6Ga/γ-Al_2O_3	0.6CoMo	9.3	2.2	0.7	2.6	0.9	0.2	0.26
CoMo/1.2Ga/γ-Al_2O_3	1.2CoMo	9.3	2.3	1.2	2.6	1.0	0.4	0.28
CoMo/1.8Ga/γ-Al_2O_3	1.8CoMo	8.8	2.3	1.8	2.5	1.0	0.6	0.29
CoMo/2.9Ga/γ-Al_2O_3	2.9CoMo	8.8	2.3	2.9	2.5	1.0	1.0	0.29
CoMo/5.9Ga/γ-Al_2O_3	5.9CoMo	8.7	2.3	6.1	2.4	1.0	2.1	0.29

[a] Atomic ratio (promoter/(promoter + Mo)).

Table 2
Rate transformation and apparent activation energy estimated in the HDS of 4,6-DMDBT over NiMo catalysts

Catalyst	r_{HDS} (10^{-8} mol s^{-1} g^{-1})				E_a (kcal mol^{-1})
	280 °C	300 °C	320 °C	340 °C	
NiMo	2.9	5.3	8.8	14.0	18
0.6NiMo	3.5	6.9	11.1	17.5	18
1.2NiMo	3.2	6.0	9.8	15.7	17
1.8NiMo	2.6	4.7	7.9	12.2	16
2.9NiMo	2.2	4.1	6.7	10.8	18
5.9NiMo	2.0	3.2	5.1	8.3	16

r_{HDS}: rate transformation of 4,6-DMDBT (Err. ±5%). Conversion under 20%.

gallium (0–5.9 wt%) at four different temperatures (280, 300, 320 and 340 °C). Compared with the NiMo reference catalyst the 0.6NiMo showed a higher activity (25%) in all temperature domains. The apparent activation energy (E_a, $R^2 \leq 0.98$) was estimated with the Arrhenius plots, giving a value of 18 kcal mol^{-1} for both catalysts. The amount of 1.2 wt% of gallium provokes a slight increase in activity of NiMo catalyst (ca. 10%) without a modification of the E_a. The catalysts with higher percentage of gallium (≥1.8 wt%) showed a lower activity compared to the reference catalyst: −5, −23, −38% for the catalysts with 1.8, 2.9, 5.9 wt% of Ga, respectively. The E_a for each catalyst are very similar for all catalysts, suggesting that the increase or decrease in activity could be related more probably with the number of catalytic sites, than with a modification of the catalytic sites.

The activity of CoMo catalysts in the HDS of 4,6-DMDBT was tested also at four different temperatures (280, 300, 320 and 340 °C). Table 3 shows the reaction rates obtained from the catalysts with different amounts of gallium (0–5.9 wt%). The 0.6CoMo catalyst showed to be more active in 40% than the reference catalyst at all temperatures domain. The catalyst 1.2CoMo was slightly more active than the CoMo reference, while the catalysts with higher content of gallium (1.8CoMo, 2.9CoMo and 5.9CoMo) presented lower activities compared to the reference catalyst.

For unpromoted MoS_2 supported catalysts, it has been proved that the activity is related to the edges of the MoS_2 nanoclusters where the active sites seems to be created; furthermore, the promoters (Co or Ni) located at the edges of the MoS_2 nanoclusters would increase the number of active sites or coordinatively unsaturated sites (CUS) created in a reaction with hydrogen [12]. In the literature, it has been widely observed that a correlation between the activity and the number of promoted edges sites exists [12,13]. On the other hand, the activity of such sulfide catalysts has been also related to the MoS_2 nanoclusters dispersion, to the interaction of these clusters with the support and as well as to the stacking of the MoS_2 slabs [15,16]. The size and the support interaction of MoS_2 have a strong influence over the high and low activity forms of the "CoMoS" phases, which were termed as type Type I and Type II CoMoS" structures. "CoMoS-I" was proposed to exist as a monolayer with strong support interaction, and difficult to be sulfided completely. "CoMoS-II" with a lower support interaction, allows the creation of more CUS.

Table 3
Rate transformation and apparent activation energy estimated in the HDS of 4,6-DMDBT over CoMo catalysts

Catalyst	r_{HDS} (10^{-8} mol s^{-1} g^{-1})				E_a (kcal mol^{-1})
	280 °C	300 °C	320 °C	340 °C	
CoMo	1.7	3.3	6.0	11.2	20
0.6CoMo	2.4	4.5	8.5	15.7	21
1.2CoMo	1.9	3.6	6.9	12.6	20
1.8CoMo	1.4	2.9	5.2	9.7	22
2.9CoMo	1.3	2.5	4.6	8.2	20
5.9CoMo	1.1	2.2	4.2	7.2	21

r_{HDS}: rate transformation of 4,6-DMDBT (Err. ±5%). Conversion under 20%.

On the basis of the above-mentioned knowledge and of the published results [5], the increase in activity of the evaluated catalysts (NiMoS and CoMoS) in the HDS of 4,6-DMDBT suggests a better MoS_2 dispersion and a better MoS_2 edge decoration (promotion). The next physicochemical characterization results will provide us valuable information, which can verify the above-mentioned facts.

3.2. X-ray diffraction (XRD)

In order to identify the possible gallium oxide entities present in the catalysts, three references were analyzed and their diffraction patterns are presented in Fig. 1. The first one, a commercial β-Ga_2O_3 phase normally obtained by the gallium nitrate [$Ga(NO_3)_3 \cdot 8H_2O$] calcination at 1200 °C, presents a high crystallinity; the second one was prepared by the calcination at 600 °C, which presents a β-Ga_2O_3 diffraction lines but with lower crystallinity, was assigned to the ε-Ga_2O_3 phase [17]; the third one was prepared also by the calcination of the same salt at 450 °C, and presents diffraction lines that correspond to the γ-Ga_2O_3 phase poorly crystallized.

In Fig. 2, the diffraction lines of alumina are found at: $2\theta = 32$, 39, 46 and 67° and correspond to the reflections (2 2 0), (3 1 1), (4 0 0) and (4 4 0), respectively. At low gallium loadings (<1.8 wt%), neither are the intensity of the alumina diffraction lines peaks affected, nor are gallium diffraction lines

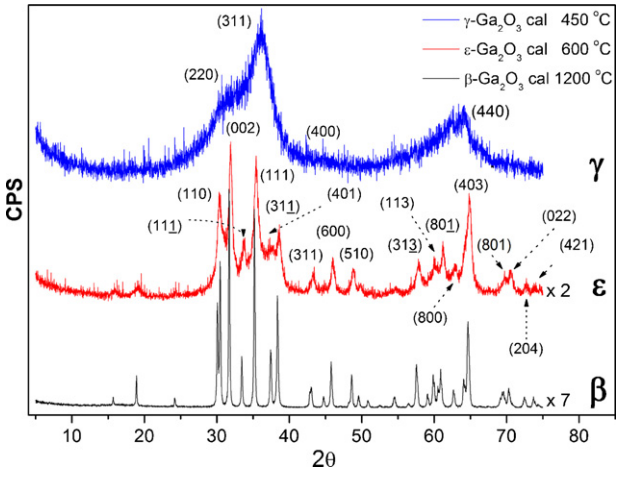

Fig. 1. XRD patterns of Ga_2O_3 prepared at three different temperatures.

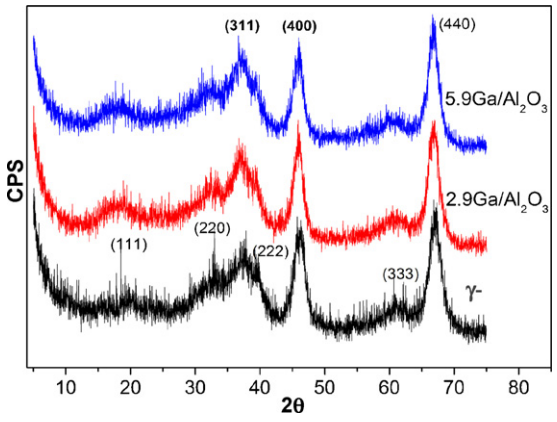

Fig. 2. XRD patterns of Ga-γ-Al_2O_3 calcined at 450 °C.

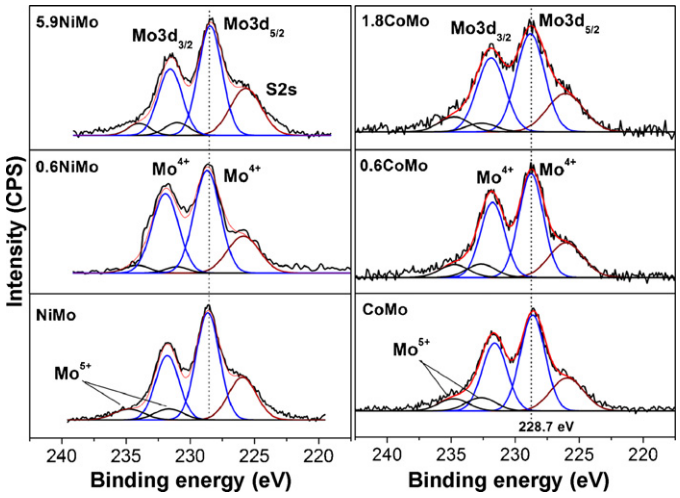

Fig. 3. Comparison of XPS spectra of the Mo 3d region for the NiMo and CoMo catalysts with different amounts of gallium. All catalysts were sulfided at 673 K.

detected (diffraction patters not presented). However, it can be observed in Fig. 2 that a gallium loading over 2.9 wt% induces slight differences. The γ-Al_2O_3 diffraction shows the next typical reflections (1 1 1), (2 2 0), (3 1 1), (2 2 2), (4 0 0), (3 3 3) and (4 4 0), and the principal variation, when gallium is present, are observed in the (3 1 1) and (4 0 0) reflections. The peak with *h l k* of (3 1 1) with 46.2% of relative intensity in non-modified alumina increases its height at 51.9% when the gallium amount is 2.9 wt%, but with a constant FWHM; this peak increases its intensity at 57.5% when the amount of gallium is 5.9 wt%. The peak with *h l k* of (4 0 0) decreases its relative intensity from 78.4 to 75.7 and 69.4% when the amount of gallium increases at 2.9 and 5.9 wt%, respectively.

Taking into account the diffraction pattern of γ-Ga_2O_3 showed in Fig. 1, it can be observed that the alumina peak increment at (3 1 1) corresponds to the (3 1 1) highest reflection of the γ-Ga_2O_3, which suggest that at high gallium loadings there could exist a contribution of γ-Ga_2O_3 bulk crystallites (≈2–4 nm). The main conclusion from these results is that at low loading of gallium, this metal is highly dispersed because the diffraction patterns did not showed any substantial modification.

3.3. X-ray photoelectron spectroscopy (XPS)

Recent studies of Ga/Al_2O_3 samples by Sulfur Temperature Programmed Reduction (TPR-S) [5], XPS [5,17], EXAFS and XANES [17] have shown that the gallium supported on alumina and calcined at 450 and 550 °C presented a tetrahedral gallium/octahedral gallium (Ga_{th}/Ga_{oh}) ratio of three for amounts of gallium lower than 3 wt% of metal. This ratio decreases as the amount of gallium increases. In Table 4, it can be observed that, between 0.6 and 1.8 wt% of gallium, the atomic ratio (Ga $2p_{3/2}$/Al 2p) is higher than that obtained by chemical analysis (ICP), suggesting that gallium is present mainly in the alumina surface.

Table 4
Atomic ratios obtained by XPS and chemical analysis (ICP)

Material	XPS (Ga $2p_{3/2}$/Al 2p)	ICP (Ga/Al)
0.6Ga-g-Al_2O_3	0.021	0.008
1.8Ga-g-Al_2O_3	0.029	0.028
5.9Ga-g-Al_2O_3	0.050	0.068

For the NiMo and CoMo sulfided catalysts with or without Ga, the Mo 3d spectrum consist of two overlapping doublets arising from the electrons of the Mo $3d_{3/2}$ (231.8 ± 0.1 eV) and Mo $3d_{5/2}$ (228.7 ± 0.1 eV), indicating that the molybdenum species exist as MoS_2 (oxidation state of 4^+) (Fig. 3). The maximum of binding energy (BE) did not change with the presence of gallium (Table 5). The appropriate spectra decomposition revealed bands of Mo^{5+}, suggesting the existence of some oxysulfide species.

Fig. 3 shows that the binding energy at 226.0 eV (±0.1) of the sulfur 2s (S 2s) did not change when gallium was present. However, the S 2s band intensity increased when the gallium amount was higher, indicating that there exist a higher amount of sulfur on the catalysts with gallium, suggesting some sulfidation of this additive.

For the reference NiMo catalyst, the band Ni $2p_{3/2}$ presented the maximum in BE at 853.9 eV (±0.1). The XPS spectra of Ni 2p slightly changed its position when Ga was present. The Ni 2p BE shifted upward by 0.2 eV (±0.1) for 0.6NiMo and downward 0.3 eV (±0.1) for 5.9NiMo with respect to the Ni 2p BE for the reference NiMo catalyst (Table 5). A similar effect is observed for the CoMo catalysts: the BE of Co $2p_{3/2}$ of the reference CoMo catalyst was observed at 778.6 eV (±0.1), while for the 0.6CoMo and 1.8CoMo catalysts the BE shifted 0.5 eV (±0.1) towards a higher BE (Table 5).

Table 5
Metals binding energies in sulfide state by XPS

Catalysts	Mo 3d (eV)	Ni $2p_{3/2}$ (eV)	Co $2p_{3/2}$ (eV)
NiMo[a]	228.7	853.9	
0.6NiMo[a]	228.7	854.1	
5.9NiMo[a]	228.6	853.6	
CoMo	228.6		778.6
0.6CoMo	228.7		779.1
1.8CoMo	228.7		779.0

[a] From Ref. [5].

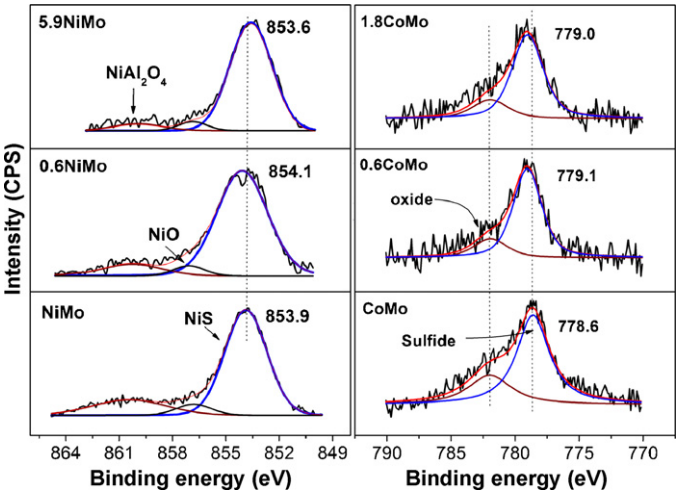

Fig. 4. Comparison of XPS spectra of Ni and Co $2p_{3/2}$ region for the NiMo and CoMo catalysts with different amounts of gallium. All catalysts were sulfided at 673 K.

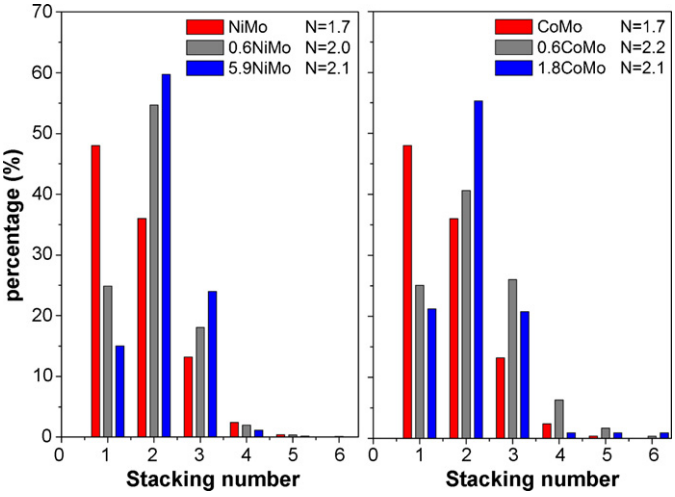

Fig. 5. MoS_2 slabs stacking for the NiMo and CoMo catalysts with different amounts of gallium.

For all NiMo catalysts, the decomposition of the Ni $2p_{3/2}$ spectra reveals a small band corresponding to the NiO with a BE of 857 eV [18]. Also it can be observed a satellite with a BE of 859.5 eV that decreased with the increase of the gallium amount; this peak has been commonly assigned to the nickel aluminate [19,20]. The same phenomena for the CoMo catalysts was noticed, the deconvolution of the Co $2p_{3/2}$ spectra reveals that the band that correspond to the cobalt in oxide state with a BE of 781 eV decreases in the presence of gallium (Fig. 4).

The upwards shift in BE of the Ni and Co $2p_{3/2}$ and the band reduction intensity of the corresponding Co^{2+} and Ni^{2+} in oxide state, suggest that the presence of gallium reduce the chemical interactions of promoter with alumina, decreasing the $NiAl_2O_4$ or $CoAl_2O_4$ species and allowing a promoter more available to be sulfided and participate in the decoration of the MoS_2 slabs.

3.4. High resolution transmission electron microscopy (TEM)

After the catalysts sulfidation process, the TEM analyses were carried out. The following results are based on the observation of about 800–1000 crystallites detected on 10 TEM micrographs for each catalyst. For each individual crystallite two parameters have been considered: the length L of the black lines, which roughly correspond to the diagonal dimension of the observed MoS_2 crystallites, and the number N of three-dimensional stacked layers, following the method of Payen et al. [21].

For the NiMo and CoMo reference catalysts, the stacking number was between 1 and 2 with an average N of 1.7 (Fig. 5), with 50% as single layers, 35% as double layers and 15% in three and four layers. The 0.6NiMo and 0.6CoMo catalysts showed an average stacking N of 2.1, which is 30% higher than the reference CoMo and NiMo catalyst. For the catalysts with 0.6, 1.8 and 5.9 wt% of gallium, the stacking was found as follow: less than 25% as single layers, 50% as double layers and 25% in three and four layers. It can be clearly observed that the gallium presence diminishes the quantity of single-layers, allowing the formation of multilayer MoS_2 slabs.

Fig. 6 shows the length distribution of the MoS_2 corresponding to the NiMo and CoMo catalysts with different amounts of additive. The reference catalysts showed slabs lengths mainly between 20, 30 and 40 Å with an average L of 36 Å (NiMo) and 33 Å (CoMo). The catalysts with 0.6 and 1.8 wt% of Ga, showed a slabs length closely similar to their corresponding reference catalyst. The average MoS_2 slabs length L for the 0.6NiMo, 0.6CoMo and 1.8CoMo were 37, 30 and 29 Å, respectively. These results suggest that gallium provokes a lower interaction between molybdenum species and support. A higher stacking at the same slab length permits the creation of more edge and corner sites, allowing the incorporation of more promoter atoms in the structures Type II ''CoMoS-II'' (NiMoS-II) [16,14]. This picture matches with the catalytic tests results.

The 5.9NiMo catalysts presented an important increment in the MoS_2 slabs length; with respect to the reference NiMo

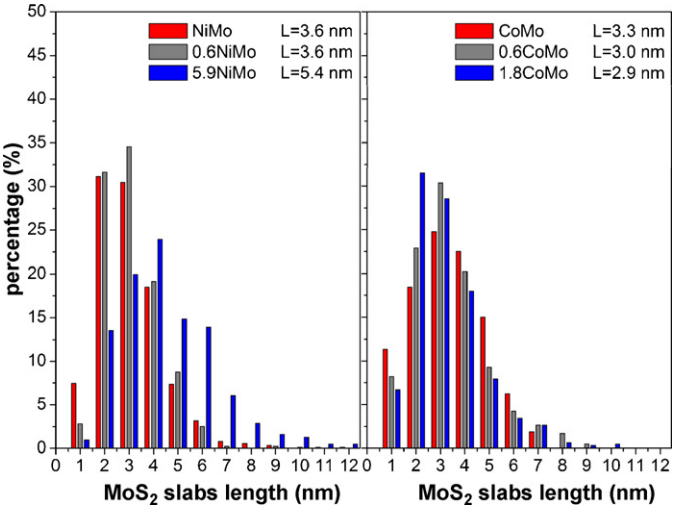

Fig. 6. MoS_2 slabs length distribution for the NiMo and CoMo catalysts with different amounts of gallium.

catalyst, the length distribution presented a Gaussian shape distribution with a maximum at 40 Å, exhibiting an average slab length of 54 Å (Fig. 6). The catalytic test over the 5.9NiMo catalyst is in agreement with the above interpretation because an important increment in the MoS_2 slab length brings as consequence a diminution of the corner and edge site, therefore lower promoted sites could be expected as the XPS results suggests.

3.5. Diffuse reflectance spectroscopy (DRS, UV–vis)

Previous TPR-S results [5] and the XPS analysis here presented suggest that gallium has an important effect over the promoter. The DRS analyses in the visible region can get valuable information related with the catalysts in oxide state, principally information about the coordination of the promoter.

In the visible region the band at 405 nm has been assigned to the octahedrally coordinated nickel ion species (Ni^{2+}_{Oh}), while the bands with wavelength between 590 and 700 nm have been assigned to the d–d electronic transition of the tetrahedrally coordinated nickel ion species (Ni^{2+}_{th}) [3,4]. Unfortunately the information about Ni^{2+}_{Oh} could not be detected because the overlapping of the 405 nm band with the Mo^{6+} in an oxide matrix band. Although, it can be observed in Fig. 7 that the absorption of the Ni^{2+}_{th} decreases with the increase of gallium. Consequently the amount of the inactive nickel species ($NiAl_2O_4$) in sulfide state decreases, suggesting that gallium is occupying the tetrahedral sites of alumina avoiding the of nickel ions in an oxide environment in tetrahedral coordination.

In a similar way for the CoMo catalysts, the spectra in the visible region present the absorption of the cobalt ion in tetrahedral coordination (Co^{2+}_{th}) and its shape is qualitatively similar to the $CoAl_2O_4$ spinel [22,23]. These bands have been largely studied in literature [4,24,25] and situated at 550, 590 and 635 nm. The intensity of this triplet diminishes with the increase in gallium concentration, where the lower signal was observed for the 5.9CoMo catalyst. On the other hand, it has been determined that the cobalt band in an oxide environment occupying octahedral sites is overlapping with the Mo^{6+} in an oxide matrix band; on the other, the formation of Co_3O_4 is discarded because the XRD analyses did not show any line that suggest the existence of Co_3O_4 crystallites. Therefore, it could be supposed that the decrease of the Co^{2+}_{th} species implies the increase Co^{2+}_{Oh} species (Fig. 8).

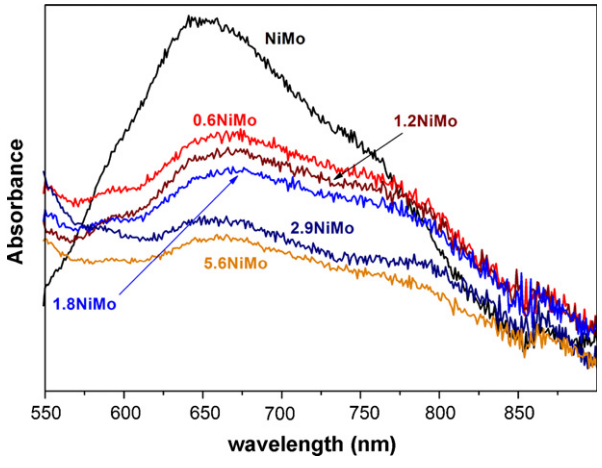

Fig. 7. DRS spectra in visible region for the NiMo catalysts with different amounts of gallium.

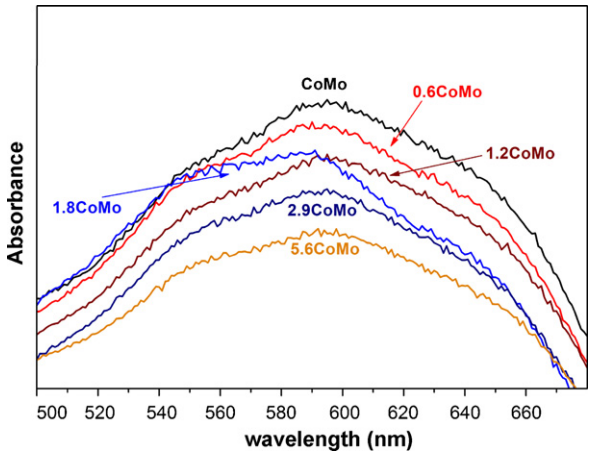

Fig. 8. DRS spectra in visible region for the CoMo catalysts with different amounts of gallium.

4. Discussion

From the results of XPS and DRS analyses, it can be argued that gallium diminished the amount of tetrahedral surrounded nickel or cobalt species ($NiAl_2O_4$/$CoAl_2O_4$) hardly sulfidable at temperature lower than 400 °C [26] and consequently these species do not participate in MoS_2 promotion. The explanation could be in terms of the gallium interaction with alumina: the addition of small quantities results in the occupation of superficial tetrahedral sites of alumina and as a result the amount of promoter octahedrally surrounded increases. For this discussion, the paper of Cimino et al. [3] is relevant, in that work it was reported that the addition of gallium to the alumina results in an increment of Ni^{2+}_{th} and Co^{2+}_{th} attributing this phenomena to the weakening of the crystal field upon the addition of gallium. If this could happen in our catalysts, the XPS results should show an increase in intensity of the oxide bands and not a decrease as shown in Fig. 4. To explain this difference, it should be pointed out that the calcination temperature used by Cimino et al. was 600 °C instead of the 450 °C used here, even more, their catalysts were calcined during 24 h instead of the 4 h used in this work. Therefore, our results of DRS suggest that the Ni^{2+}_{th} or Co^{2+}_{th} species decrease implying that the Ni^{2+}_{Oh} or Co^{2+}_{Oh} species increase, this can be inferred since the TEM analyses in the sulfide state did not reveal any signal of bulk Ni_3S_2 or Co_9S_8 crystallites. Furthermore, the XPS results showed [5] an homogeneous dispersion of the Ni^{2+} or Co^{2+} ions, this let us to consider that there exist more octahedral species (Ni^{2+}_{Oh} or Co^{2+}_{Oh}) easy to be sulfided and ready to participate in the decoration of the active phase CoMoS or NiMoS. In the literature a similar effect has been observed when small amounts of Zn [27–30] or Mg [27,31,32] were added to the alumina before the impregnation

of the Mo and Ni. This metals (Me) can form spinel species type $MeAl_2O_4$, which decrease the amount of Ni or Co inside $NiAl_2O_4$ or $CoAl_2O_4$. Consequently, more Ni or Co could be involved in the formation of promoted sites and the HDS activity is increased.

From the discussion above presented, and taking into account the TEM results, it can be suggested that gallium also modifies the interaction of Mo with alumina since the stacking MoS_2 slabs change in the presence of gallium. The XPS suggests that there exist more nickel or cobalt promoting the MoS_2 slabs, since the BE of Ni or Co $2p^{3/2}$ shift towards higher energies, which means that there exist more active phases, commonly called NiMoS or CoMoS. When the amount of gallium is less than 1.2 wt%, it can be inferred that there exist more promotion of the MoS_2 slabs. Consequently, this results are reflected in an increment of 20% for the 0.6NiMo and 40% for the 0.6CoMo in the HDS of 4,6-DMDBT in a continuous flow reactor.

5. Conclusions

At low amounts of gallium, there exist more sulfidable well-dispersed Ni or Co species that participate in the decoration of the ''NiMoS'' or ''CoMoS'' phase leading to an increase in the HDS activity. This effect might be caused by the existence of gallium in tetrahedral coordination over the alumina sites, which enhances the sulfidability of MoO_3 and decreases the formation of $NiAl_2O_4$ or $CoAl_2O_4$ with the promoter in tetrahedral coordination.

Acknowledgments

This research was performed under the auspices of the Institut de Recherches sur la Catalyse, Instituto Mexicano del Petróleo, and CONACYT (Project 42204-Y). One of us (E. Altamirano) is grateful to the Postgraduate Cooperation Program (PCP France-Mexico) and to the CONACyT for a graduate scholarship.

References

[1] H. Topsøe, B.S. Clausen, F.E. Massoth, in: J.R. Anderson, M. Boudart (Eds.), Hydrotreating Catalysis Science and Technology, Springer, Berlin, 1996.
[2] T. Kabe, A. Ishihara, W. Qian, Hydrodesulfurization and Hydrodenitrogenation, Wiley-VCH, Japan, 1999.
[3] A. Cimino, M.L. Jacono, M. Schiavello, J. Phys. Chem. 79 (1975) 243.
[4] M.L. Jacono, M. Schiavelo, V.H.J. de Beer, G. Minelli, J. Phys. Chem. 81 (1977) 6.
[5] E. Altamirano, J.A. de los Reyes, F. Murrieta, M. Vrinat, J. Catal. 235 (2005) 403.
[6] H. Morishige, Y. Akai, Bull. Soc. Chim. Belg. 104 (1995) 4.
[7] D. Li, T. Sato, M. Imamura, H. Shimada, A. Nishijima, J. Catal. 170 (1997) 357.
[8] W.O. Flego, Parker Jr., Appl. Catal. A 185 (1999) 137.
[9] D. Ferdous, A.K. Dalai, J. Adjaye, Appl. Catal. A 260 (2004) 137.
[10] D. Li, T. Sato, M. Imamura, H. Shimada, A. Nishijima, Appl. Catal. B 16 (1998) 255.
[11] M. Lewandowski, Z. Sarbak, Fuel 79 (2000) 487.
[12] R. Prins, V.H.J. de Beer, G.A. Somorjai, Catal. Rev. Sci. Eng. 31 (1989) 1.
[13] J. Grimblot, Catal. Today 41 (1998) 111.
[14] H. Topsøe, B. Hinnemann, J.K. Norskov, J.V. Lauritsen, F. Besenbacher, P.L. Hansen, G. Hytoft, R.G. Egeberg, K. Knudsen, Catal. Today 107 (2005) 12.
[15] J. Miciukiewicz, Appl. Catal. 49 (1989) 247.
[16] R. Candia, O. Sorensen, J. Villandsen, N. Topsøe, B.S. Clausen, H. Topsøe, Bull. Soc. Chim. Belg. 93 (1984) 763.
[17] K. Shimizu, M. Takamatsu, K. Nishi, H. Yoshida, A. Satsuma, T. Tanaka, S. Yoshida, T. Hattori, J. Phys. Chem. B 103 (1998) 1542.
[18] U.S. Ozkan, L. Zhang, S. Ni, E. Moctezuma, J. Catal. 148 (1994) 181.
[19] P. Salagre, J.L.G. Fierro, F. Medina, J.E. Sueiras, J. Mol. Catal. A 106 (1996) 125.
[20] K.T. Ng, D.M. Hercules, J. Phys. Chem. 80 (1976) 2094.
[21] E. Payen, R. Hubaut, S. Kasztelan, O. Poulet, J. Grimblot, J. Catal. 147 (1994) 123.
[22] R.L. Chin, D.M. Hercules, J. Phys. Chem. 86 (1982) 360.
[23] R.B. Greegor, F.W. Lytle, R.L. Chin, D.M. Hercules, J. Phys. Chem. 85 (1981) 1232.
[24] M. Vrinat, D. Letourneur, R. Bacaud, V. Harlé, B. Jouguet, C. Leclercq, in: B. Delmon, G.F. Froment, P. Grange (Eds.), Hydrotreating and Hydrocracking of Oil Fractions, Elsevier, Amsterdam, 1999, p. 153.
[25] Ch. Papadopoulou, J. Vakros, H.K. Matralis, Ch. Kordulis, A. Lycourghiotis, J. Colloid Interface Sci. 261 (2003) 146.
[26] B. Scheffer, N.J.J. Dekker, P.J. Mangnus, J.A. Moulijn, J. Catal. 121 (1990) 31.
[27] G. Muralidhar, F.E. Massoth, J. Shabtai, J. Catal. 85 (1984) 44.
[28] C.L. Kibby, H.E. Swift, J. Catal. 45 (1976) 231.
[29] V.H.J. De Beer, T.H.M. Van Sint Fiet, G.H.A.M. Van Der Steen, A.C. Zwaga, G.C.A. Schuit, J. Catal. 35 (1974) 297.
[30] P.J. Mangnus, Characterization of hydrotreating catalysts with temperature programmed techniques, Ph.D. Thesis, University of Amsterdam, The Netherlands, 1991 (Chapter 9).
[31] A.R. Saini, B.G. Johnson, F.E. Massoth, Appl. Catal. 40 (1988) 157.
[32] K. Jirátová, M. Kraus, Appl. Catal. 27 (1986) 21.